

# Rainbow and glory scattering in Coulomb trajectories starting from a point in space

I Samengo and R O Barrachina†

Comisión Nacional de Energía Atómica, Centro Atómico Bariloche and Instituto Balseiro‡, 8400 Bariloche, Río Negro, Argentina

Received 26 April 1994

**Abstract.** We have studied the family of orbits encountered when particles are emitted in all directions from a point source, in the presence of a Coulomb potential whose centre is displaced with respect to the source.

This is a simple system in which all the calculations can be done analytically. We found that, depending on the sign of the potential, the effective cross section exhibits glory or rainbow divergences. We provide an approach for studying these effects which is suited for a course on classical mechanics.

**Resumen.** Hemos estudiado la familia de trayectorias de un conjunto de partículas emitidas en todas direcciones por una fuente puntual que se encuentra desplazada respecto de un centro de potencial Coulombiano. Este es un sistema simple, en el que todos los cálculos pueden realizarse analíticamente. Encontramos que, dependiendo del signo del potencial, la sección eficaz efectiva presenta divergencias de Gloria o Arco Iris. Encaramos el estudio de estos efectos desde un punto de vista apropiado para un curso de mecánica clásica.

## 1. Introduction

There are a number of interesting aspects concerning the treatment of trajectories and scattering processes in a central force field which are commonly omitted in the standard textbooks on classical mechanics (Goldstein 1965, Landau and Lifshitz 1976). For instance, it has been pointed out (Caplan *et al* 1977) that usually students do not clearly understand the relation between the constants of integration of the problem and the starting conditions which specify one particular evolution. In this context, the calculation of an orbit from its initial conditions seems to be a pedagogically sound but neglected exercise.

In this paper, we shall study the family of orbits travelled by particles subject to an inverse square law of force, all starting from a fixed point in space with the same initial velocity. This system shows many interesting properties, as described by Laporte in his article of 1970 (Laporte 1970). Furthermore, this problem is by no means academic since, besides

being obviously related to the launching of satellites from a space-based position (Caplan *et al* 1977, Laporte 1970), it represents a physical situation which occurs in atomic physics. Actually, we first became interested in the subject of this paper while studying the decay of an autoionizing state formed by the impact of a slow charged ion. In a semiclassical treatment of this problem, the trajectory of the emitted electron is affected by the post-collision interaction with the Coulomb field of the outgoing projectile (Swenson *et al* 1991, Barrachina and Macek 1989). When analysed in a moving reference frame attached to the projectile, this problem can be reduced to the one discussed in this paper.

Here we show that the family of classical Coulomb orbits starting from a point in space provides an elegant framework for the introduction of the glory and rainbow effects in scattering processes. Both effects, besides producing a great fascination, convey a considerable pedagogical interest since they introduce the student into different areas of physics of increasing complexity, from simple classical trajectories and geometrical optics, to wave interference (Bryant and Jarmie 1974, Walker 1976, Nussenzveig 1977, Gillis *et al* 1982). The calculations, not being too lengthy or difficult, are very well suited for an intermediate or advanced course on classical

†Also member of the Consejo Nacional de Investigaciones Científicas y Técnicas, Argentina.

‡Comisión Nacional de Energía Atómica and Universidad de Cuyo, Argentina.

mechanics. Furthermore, all the results are given by simple analytical expressions.

In section 2 we shall describe some geometrical features of the family of Coulomb trajectories travelled by particles emitted from a fixed point in space. Afterwards we derive, in section 3, the dispersion function which relates the deflection angle to the initial conditions at the launching point. This dispersion function is used in section 4 to calculate an effective cross section which exhibits rainbow and glory divergences. Finally, in sections 5 and 6 we discuss how these rainbow and glory effects relate to analogous phenomena in atomic, nuclear and optical physics.

### 2. Coulomb trajectories starting from a point in space

Let us consider the case of a particle of mass  $m$  which is released with initial velocity  $v_0$  from a point  $P$  which is at a given distance  $R$  from a force centre with an inverse square dependence on the distance. The initial velocity  $v_0$  makes an angle  $\alpha$  with an axis through the starting point and the force centre, as shown in figure 1. This angle  $\alpha$  is measured counter-clockwise.

Let  $r$  and  $\theta$  be plane polar coordinates of the particle (as shown in figure 1), the origin  $O$  being at the force centre. The potential energy is given by  $V(r) = k/r$ , which applies for both the gravitational and the Coulomb force problem. If  $k < 0$  we shall be dealing with an attractive potential, and  $k > 0$  stands for a repulsive one. Since this is a central

**Figure 1.** Geometrical situation at time  $t$  after the projectile of mass  $m$  has been emitted with velocity  $v_0$  from a point  $P$  at a distance  $R$  from a force centre at  $O$  with potential  $V(r) = k/r$ . The coordinates  $r$  and  $\theta$  define the position of the particle at time  $t$ .

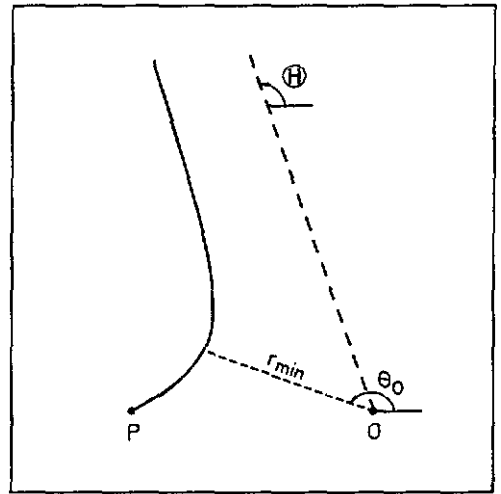
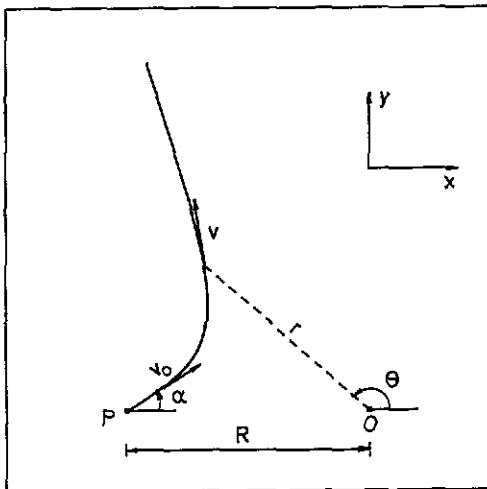


**Figure 2.** Distance of minimum approach  $r_{min}$  and angle  $\theta_0$ , which define the position of the perihelion. We have also pictured the deflection angle  $\Theta$ , defined as  $\lim_{r \rightarrow +\infty} \theta$ .

potential, the angular momentum  $L$  is conserved and the orbit is planar. The equation of the trajectory reads (Caplan *et al* 1977)

$$\frac{1}{r} = -\frac{km}{L^2} + \sqrt{(km/L^2)^2 + 2mE/L^2} \cos(\theta - \theta_0). \tag{1}$$

The phase angle  $\theta_0$  defines the direction of a vector which points from the force centre to the perihelion, as shown in figure 2. The orbit is symmetrical about this direction, which is fixed by the initial conditions of launch (Laporte 1970)

$$\cot \theta_0 = \left(1 + \frac{mkR}{L^2}\right) \tan \alpha. \tag{2}$$

Upon replacing the energy

$$E = \frac{1}{2}mv_0^2 + \frac{k}{R} \tag{3}$$

and the angular momentum

$$L = -mRv_0 \sin \alpha, \tag{4}$$

the following result is obtained:

$$\frac{R}{r} \sin^2 \alpha = -\frac{A}{2} (1 + \cos \theta) + \sin \alpha \sin(\theta - \alpha), \tag{5}$$

where the dimensionless parameter

$$A = \frac{2k}{mv_0^2 R} \tag{6}$$

represents the ratio between the potential and kinetic energies at the moment of emission. We see in equation (5) that each particular orbit is fully

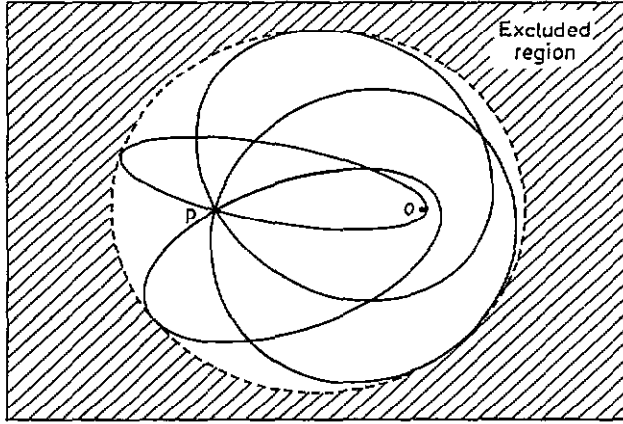


**Figure 3.** Family of orbits for the situation of figure 1 with  $A = 2k/mv_0^2R = -3$ . The envelope of all these elliptic trajectories is also an ellipse, whose two foci are the attractive centre O and the point of release P.

characterized by the parameters  $A$  and  $\alpha$ . The eccentricity reads (Landau and Lifshitz 1976)

$$\epsilon = \sqrt{1 + \frac{2EL^2}{mk^2}} = \sqrt{1 + \frac{4(A+1)}{A^2} \sin^2 \alpha}. \quad (7)$$

For the case of an attractive potential, i.e.  $k < 0$ , the orbit is an ellipse if the initial conditions satisfy  $A < -1$ . If the initial velocity is increased so that  $A = -1$  the orbit becomes a parabola with its vertex in the point of release. For  $A > -1$ , the orbit is a hyperbola. Finally, when the potential is repulsive, all possible orbits are hyperbolic.

The problem of Kepler ellipses starting from a point in space has been previously analysed by other authors (Caplan *et al* 1977, Laporte 1970). Here we shall be studying a scattering problem, and therefore, the orbits are expected to go out into infinity. This means that we will only deal with the case  $\epsilon \geq 1$ . Thus, we will consider the case of hyperbolic or parabolic orbits which at infinity have a velocity

$$v_\infty = v_0 \sqrt{1 + A}. \quad (8)$$

Let us now determine the accessible region in space for all the orbits starting at a given point with equal initial kinetic energy  $mv_0^2/2$ , but different emission angles  $\alpha$ . This region is bounded by a curve  $r_b(\theta)$ , which is called the *envelope* of the trajectories. In order to obtain this curve (Warner and Huttar 1991), we consider that for each value of  $\theta$ , the radius  $r$  in equation (5) defines, as a function of  $\alpha$ , all the accessible points in that particular direction. Thus, to determine the boundary point  $r_b$  for a given  $\theta$ , we require  $(\partial r / \partial \alpha)|_\theta = 0$  in equation (5). We obtain

$$\tan \alpha = A \frac{1 + \cos \theta}{\sin \theta}, \quad (9)$$

which, upon substitution into equation (5), yields

$$\frac{R}{r_b} = \frac{1}{2A} [1 - A^2 - (1 + A)^2 \cos \theta]. \quad (10)$$

This equation is well defined except for the interval  $-1 < A < 0$ . But in this case, the trajectories are hyperbolae around an attractive centre, and there is no excluded region in space. For  $A < -1$ , the previous equation defines the envelope of all the orbital ellipses, as shown in figure 3. This envelope is itself an ellipse, whose two foci are the attractive centre O and the point of release P (Caplan *et al* 1977). Finally, in the case of a repulsive potential (i.e.  $k > 0$ , which means  $A > 0$ ), we see in figure 4 that the envelope of all the hyperbolic trajectories is also a hyperbola with vertex at the starting point and focus at the force centre. As the point of release moves towards infinity, i.e.  $R \rightarrow \infty$ , this hyperbola degenerates into the familiar parabolic caustic (Warner and Huttar 1991, Adolph *et al* 1972) which one encounters when discussing the Rutherford scattering problem

$$\frac{1}{r_b} = \frac{mv_0^2}{4k} (1 - \cos \theta). \quad (11)$$

For future reference, we mention that in the case of a repulsive potential (i.e.  $k > 0$ ) equation (10) can be written in the following way

$$\frac{R}{r_b} = \frac{2}{\sin^2 \Theta_R} (\cos \Theta_R - \cos \theta), \quad (12)$$

with

$$\cos \Theta_R = \frac{1 - A}{1 + A}. \quad (13)$$

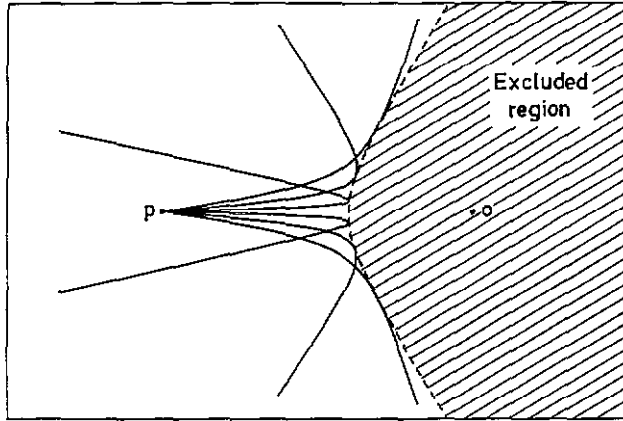
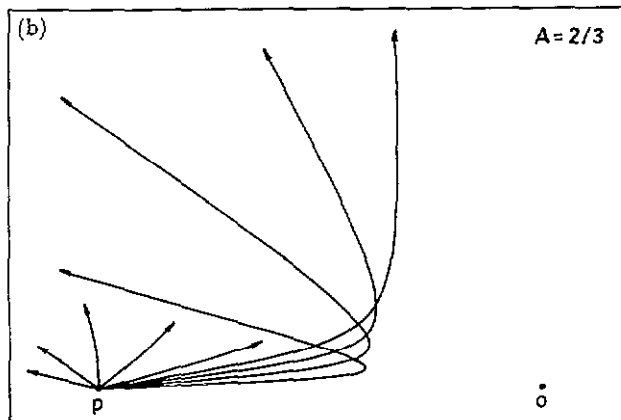
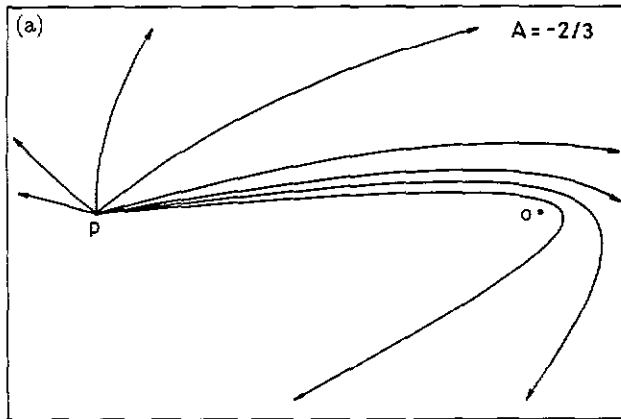


**Figure 4.** Family of orbits for the situation of figure 1 with  $A = 2k/mv_0^2R = \frac{2}{3}$ . The excluded region is limited by a hyperboloid of revolution with vertex at the starting point P and focus at the force centre O.

**Figure 5.** Families of orbits for particles having identical initial velocity, but varying emission angle  $\alpha$  for the cases: (a)  $A = 2k/mv_0^2R = -\frac{2}{3}$  and (b)  $A = 2k/mv_0^2R = \frac{2}{3}$ .



This angle  $\Theta_R$ , which can also be expressed in terms of the initial and final velocities  $v_0$  and  $v_\infty$  as

$$\Theta_R = 2 \arccos\left(\frac{v_0}{v_\infty}\right), \quad (14)$$

defines the aperture of the shadow zone. Namely, the possible deflections of the particle lie within the range of angles from  $\Theta_R$  to  $\pi$ .

### 3. Dispersion function

Let us now consider the case of particles ejected from the release point P in all directions, with initial velocity  $v_0$ . We will consider the case of open trajectories, i.e.  $A > -1$ . Figure 5 shows two families of such trajectories for (a) an attractive potential ( $A = -2/3$ ) and (b) a repulsive potential ( $A = 2/3$ ). In the limit  $r \rightarrow \infty$ , equation (5) provides the final deflection angle (see figure 2)  $\Theta = \lim_{r \rightarrow \infty} \theta$  in terms of the initial emission angle  $\alpha$ . It reads

$$\cos \Theta = -1 + \frac{\sin^2 \alpha}{1 + \frac{1}{2}A - \sqrt{1 + A \cos \alpha}}, \quad (15)$$

or, in terms of the final velocity  $v_\infty$ ,

$$\cos \Theta = 1 - \frac{2(v_0 \cos \alpha - v_\infty)^2}{v_0^2 + v_\infty^2 - 2v_0 v_\infty \cos \alpha}. \quad (16)$$

Since the potential is symmetrical around an axis through the starting point and the force centre, positive and negative values of  $\Theta$  are physically indistinguishable. Therefore we adopt the standard technique of restricting the deflection angle  $\Theta$  to the range  $0 \leq \Theta \leq \pi$ , which removes the indeterminacy in equation (16).

Figure 6 shows the dispersion function  $\Theta(\alpha)$  for different values of the parameter  $A = 2k/mv_0^2 R = (v_\infty/v_0)^2 - 1$ . For a very weak potential (i.e. for a small value of  $|A|$ ) the trajectories are almost straight lines and  $\Theta \approx \alpha$ , except when the particle is emitted towards the force centre within a cone with aperture  $\Delta\alpha$  of the order of  $|A|$ . This observation is valid for both an attractive and a repulsive potential. In the limiting case of  $A = -1$ , we have parabolic orbits and  $\Theta = |\pi - 2\alpha|$ . On the other hand, for a very strong repulsive potential, i.e.  $A \rightarrow \infty$ , we have  $\Theta \approx \pi$ . This means that all the particles are backscattered into a cone with aperture  $\Delta\Theta$  of the order of  $|A|^{-1/2}$ .

### 4. Effective cross section

We see in figure 6 that the relation between  $\Theta$  and  $\alpha$  is not one-to-one, namely there are two different initial emission angles  $\alpha_\pm$  which define trajectories with the same deflection angle  $\Theta$ . Starting from

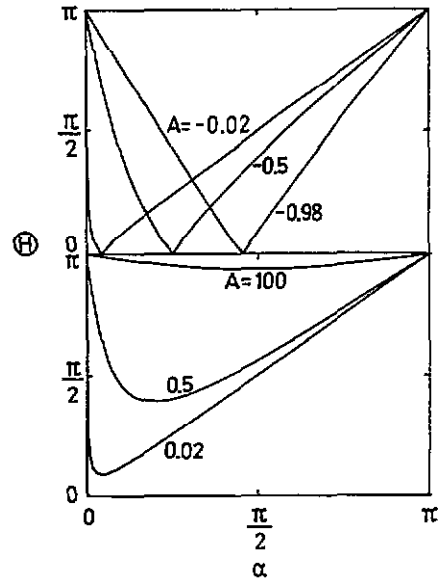


Figure 6. Dispersion function  $\Theta(\alpha)$ , as given by equation (15), for different values of the parameter  $A = 2k/mv_0^2 R$ .

equation (16) we find

$$2v_0 \cos \alpha_\pm = v_\infty(1 + \cos \Theta) \pm \sqrt{v_\infty^2(1 - \cos \Theta)^2 - 2(v_\infty^2 - v_0^2)(1 - \cos \Theta)}. \quad (17)$$

Now let us consider not the trajectory of a single particle but the scattering of a spherically outgoing beam of identical particles flying in all directions from the point of release. Let  $I_0$  be the number of these particles emitted per unit time and solid angle from the starting point O. Since the relation between  $\alpha$  and  $\Theta$  is not one-to-one, the flux  $2\pi I_\infty d(\cos \Theta)$  of particles scattered through angles between  $\Theta$  and  $\Theta + d\Theta$  is made up of two different contributions from particles whose initial emission angles are around  $\alpha_+(\Theta)$  and  $\alpha_-(\Theta)$ , i.e.

$$2\pi I_\infty d(\cos \Theta) = 2\pi I_0 d(\cos \alpha_+) + 2\pi I_0 d(\cos \alpha_-). \quad (18)$$

We define an effective cross section  $\sigma(\Theta)$  as the ratio

$$\sigma(\Theta) = \frac{I_\infty}{I_0} = \left| \frac{d(\cos \alpha)}{d(\cos \Theta)} \right|_{\alpha_+} + \left| \frac{d(\cos \alpha)}{d(\cos \Theta)} \right|_{\alpha_-}. \quad (19)$$

This definition is operationally equivalent to the standard one for the scattering of a beam of particles by a force centre (Landau and Lifshitz 1976),

$$\frac{d\sigma}{d\Omega} = \sum_i \left| \rho_i \frac{d\rho_i}{d(\cos \Theta)} \right|, \quad (20)$$

except for the fact that here the trajectories are parametrized not by an impact parameter  $\rho$  but by

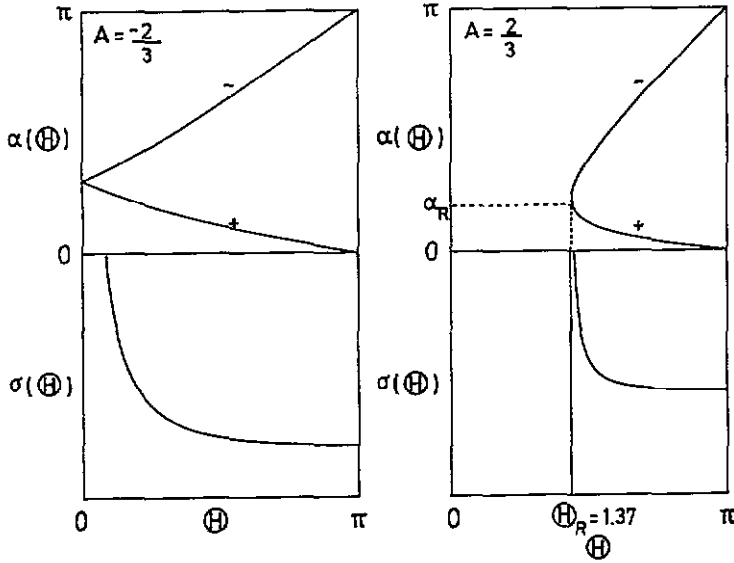


**Figure 7.** Relation  $\alpha(\Theta)$  between the emission and deflection angles, as given by equation (17) and the corresponding effective cross section  $\sigma(\Theta)$  in equation (22) for the cases  $A = -\frac{2}{3}$  and  $A = \frac{2}{3}$ .

an initial emission angle  $\alpha$  which makes our  $\sigma(\Theta)$  a dimensionless quantity. Actually, the differential cross section (20) can be easily related to our definition (22) in the limit  $R \rightarrow \infty$ , as is shown in the appendix.

By differentiating equation (17) with respect to  $\cos \Theta$ , the following expressions for both contributions to the effective cross section (19) are obtained:

$$\sigma_{\pm}(\Theta) = \frac{|d(\cos \alpha_{\pm})|}{|d(\cos \Theta)|} = \frac{1}{2v_0} \left[ \frac{v_0^2 - v_{\infty}^2 \cos \Theta}{\sqrt{2v_0^2(1 - \cos \Theta) - v_{\infty}^2 \sin^2 \Theta}} \mp v_{\infty} \right] \quad (21)$$

These expressions are meaningless when the square root becomes imaginary. However, it can be seen that this situation only arises in the repulsive case ( $k > 0$ ), whenever  $\Theta < 2 \arccos(v_0/v_{\infty})$ . These angles correspond to the shadow region where there are no scattered particles. Therefore, the effective cross section can be written as

$$\sigma(\Theta) = \sigma_+(\Theta) + \sigma_-(\Theta) = \frac{1}{v_0} \frac{v_0^2 - v_{\infty}^2 \cos \Theta}{\sqrt{2v_0^2(1 - \cos \Theta) - v_{\infty}^2 \sin^2 \Theta}} \times H[(v_0^2 - v_{\infty}^2 \cos \Theta) - |v_0^2 - v_{\infty}^2|] \quad (22)$$

with  $H(x)$  being the Heaviside step function, i.e.  $H(x) = 1$  for  $x \geq 0$ , and  $H(x) = 0$  for  $x < 0$ .

On integrating over all angles, we find the total cross section

$$\sigma_T = 2\pi \int_0^{\pi} \sigma(\Theta) \sin \Theta d\Theta = 4\pi. \quad (23)$$

As expected, it represents the solid angle into which the particle has to be emitted in order to be scattered.

In figure 7 we show the relation  $\alpha(\Theta)$  between the emission and deflection angles, as given by equation (17), and the corresponding effective cross section  $\sigma(\Theta)$  for the cases of an attractive potential such that  $A = -\frac{2}{3}$ , and a repulsive one with  $A = \frac{2}{3}$ . There we can see that the cross section  $\sigma(\Theta)$  diverges at  $\Theta = 0$  and  $\Theta = 2 \arccos(v_0/v_{\infty})$ , respectively. The first case, which corresponds to the so-called forward glory scattering, will be analysed in section 7. In the second case, the angle  $\Theta_R$  defined in equation (14), gives the aperture of the excluded region into which none of the hyperbolic orbits penetrates. As will be shown in the following section, this divergence represents a rainbow scattering effect.

### 5. Rainbow effect

In the previous section we have found that the effective cross section (22) diverges at an angle  $\Theta_R = 2 \arccos(v_0/v_{\infty})$  when the potential is repulsive, i.e.  $k > 0$ . The cause of this divergence lies in the fact that, as the emission angle  $\alpha$  is varied from 0 to  $\pi$ ,

the deflection angle  $\Theta$  diminishes from  $\pi$  to a minimum value  $\Theta_R$ , and afterwards increases again. The effective cross section  $\sigma(\Theta)$ , being proportional to  $(d\Theta/d\alpha)^{-1}$ , becomes infinite at precisely this minimum angle  $\Theta_R$ . As is shown below, this phenomenon is geometrically analogous to what happens to a beam of light rays scattered by a water droplet, leading to the formation of an optical rainbow. Hence, this kind of divergence in a classical cross section is known as *rainbow scattering* (Ford and Wheeler 1959).

The rainbow in the sky was one of the first physical phenomena to be studied scientifically. The references Nussenzweig (1977), Boyer (1959) and Greenler (1980) are warmly recommended for the reader interested in the historical development of this subject. The first satisfactory explanation for the rainbow scattering of sunlight by water droplets in the atmosphere was given by René Descartes in a treatise published in 1637. He discovered that a light ray which, upon entering a droplet of water, suffers one internal reflection, emerges with a deflection angle  $\Theta$  which shows an extremum  $\Theta_R$  as a function of its impact parameter  $\rho$  with respect to the centre of the drop. As the intensity is proportional to  $(d\Theta/d\rho)^{-1}$ , this extremum gives rise to a singularity in the intensity, producing a clear bow in the sky. The colours of the rainbow were explained thirty years later by Newton in his prism experiment. Each colour has a different index of refraction by water and, therefore, a slightly different rainbow angle.

In atomic scattering, singularities in the classical cross section were first predicted by Firsov in 1953 (Firsov 1953) and independently by Manson in 1957 (Manson 1957). The analogy between these singularities and the optical rainbow was pointed out by Ford and Wheeler in 1959 (Ford and Wheeler 1959). Since these early papers and the first observation by Beck (Beck *et al* 1979), the rainbow effect has been widely observed in atomic collisions (Kleyn 1987). These atomic rainbows are again due to the fact that, whenever the dispersion relation  $\Theta(\rho)$  shows an extremum, there is a singularity in the scattering cross section (20) of the form (McDowell and Coleman 1970)

$$\frac{d\sigma}{d\Theta} \propto \frac{1}{\sqrt{|\Theta - \Theta_R|}} \quad (24)$$

In a quantum mechanical or semiclassical approach, this classical singularity becomes a maximum at smaller scattering angles. Furthermore, interference effects occur in the form of supernumerary rainbows (Ford and Wheeler 1959).

In their paper of 1959, Ford and Wheeler (Ford and Wheeler 1959) also discussed the possibility of observing rainbow phenomena in nuclear physics. A structureless fall-off observed in the angular distributions of some nucleus-nucleus elastic scattering experiments was interpreted as the fingerprint of a

'nuclear rainbow' effect (DeVris *et al* 1977). However, since the probability for reactive processes is generally considerable, it was not clear whether this fall-off was indeed associated with the dark side of a rainbow or due to absorption. Actually, it has been pointed out (McVoy and Satchler 1984) that the use of the 'rainbow' terminology, natural as it was in atomic physics, is inappropriate to describe much of the above experiments, except for those referred to the scattering of light ions at sufficiently high energies (Put and Paans 1977).

Let us note that the basic idea underlying the rainbow effect is that of a singularity in the Jacobian relating the initial and final parameters of a scattering event. Actually, rainbow phenomena have been identified in different scattering events other than the angular deflection by a central potential. For instance, when a molecule is scattered by a surface, rotational modes  $L$  are expected to be excited, except when the internuclear axis of the molecule is parallel or normal to the surface. Thus, the excitation probability as a function of the initial orientation  $\alpha$  of the molecule will exhibit at least one extremum, i.e.  $\partial L/\partial\alpha = 0$ . This effect is called rotational rainbow (Kleyn 1987). Similar rotational rainbows have also been reported in atom-molecule collisions (Beck *et al* 1979). This concept of a rainbow effect is also applicable in surface scattering and in a wealth of other scattering situations as the so-called orientational, multiple collision and vibrationally induced rainbows (Kleyn 1987).

After this succinct review of rainbow scattering, let us now analyse our effective cross section (22) for the case of a repulsive potential. Since  $v_0 < v_\infty$ , the cross section is zero for  $\Theta < \Theta_R$ . Therefore, we see that our result shows a *zone of darkness*. This is also encountered in the optical rainbow: the sky shows a dark band between the primary and secondary light rainbows, called *Alexander's dark band*. The explanation is identical in both cases, i.e. there is no contribution to the intensity in this zone because that would represent an angle of deflection smaller than  $\Theta_R$ , which is itself the angle of minimum deviation. Furthermore, we see in equation (22) that, as for the case of the rainbow scattering of sunlight by water droplets, the effective cross section  $\sigma(\Theta)$ , which is proportional to  $(d\Theta/d\alpha)^{-1}$ , diverges at this angle  $\Theta_R$ . Actually, for  $\Theta$  close to  $\Theta_R$  the cross section behaves like

$$\sigma(\Theta) \approx \frac{\sqrt{\tan \alpha_R}}{2 \cos \alpha_R} \frac{1}{\sqrt{|\Theta - \Theta_R|}} H(\Theta - \Theta_R). \quad (25)$$

Regarding these similarities we adopt the common practice (Ford and Wheeler 1959) of taking over the language of optics and speak of a *rainbow scattering effect*.

Usually, rainbows are due to a balance of counteracting forces. This means that they are met in the case of potentials which are repulsive in one part of space and attractive in some other. This condition

is necessary if the scattering is such that the particles come from infinity. There is an extremal trajectory for which the angular deflection due to one force is not yet strongly affected by the other. At this rainbow trajectory, the cross section diverges. In our case, the same effect is achieved by only one force. The difference lies in the fact that our initial distribution is not a parallel beam, but a spherically outgoing flux.

## 6. Forward glory effect

The so-called *forward glory effect* occurs in classical scattering processes whenever the dispersion function  $\Theta(\rho)$  passes smoothly through 0 as a function of the impact parameter  $\rho$  (Ford and Wheeler 1959). The cross section (20) diverges since  $\sin \Theta$  vanishes while  $\rho$  and  $d\Theta/d\rho$  remain finite. In our case, we see in figure 7 and equation (22) that a similar divergence of  $\sigma(\Theta)$  occurs at  $\Theta = 0$ . The explanation of this divergence is identical, except for the fact that the role of the impact parameter  $\rho$  is played by the initial emission angle  $\alpha$ .

From equation (17) we see that the deflection angle  $\Theta = 0$  corresponds to the so-called *glory trajectory* characterized by an initial emission angle  $\alpha_G = \arccos(v_\infty/v_0)$ . For small values of  $\Theta$ , the cross section behaves as

$$\sigma(\Theta) \approx \frac{\sin \alpha_G}{\Theta}. \quad (26)$$

Physically, this divergence occurs since the attractive potential focuses those trajectories with initial emission angles  $\alpha$  around  $\alpha_G$  into the forward direction. In this context, the term *Coulomb focusing* has been recently used to describe an effect of this kind observed in atomic scattering experiments (Swenson *et al* 1991). Let us note, however, that neither this glory effect, nor the rainbow scattering described in the previous section, are exclusive of a Coulomb interaction. Actually both effects can equally occur with practically any other central potential, provided the scattered particles emerge from a point source. Hence, glory scattering seems to be a much more adequate name for describing this phenomenon.

In the scattering of a beam of particles by a force centre, this forward glory divergence, if present, is usually masked by the contribution from large impact parameters. This masking effect is obviously absent in our case, where there are no other trajectories which end up in the forward direction, except for the glory trajectory.

It is clear that a similar divergence of the scattering cross section (20), called *backward glory*, could eventually occur when  $\Theta = \pi$ . In the scattering of a beam of particles by a force centre, this backward glory divergence is much more easily observed than the corresponding effect in the forward direction, since

it is not usually masked by other spurious contributions. In our case, however, no backward glory divergence occurs, since the initial solid angle  $2\pi d(\cos \alpha)$  in (19) vanishes together with  $2\pi d(\cos \Theta)$  when  $\Theta = \pi$ . Therefore, the effective cross section  $\sigma(\Theta)$  remains finite in the backward direction. It is the similarity of the backward glory phenomenon with the optical glory which prompted Ford and Wheeler to coin the term 'glory scattering', even though the correspondence between both mechanisms is not as clear as for the rainbow phenomenon (Bryant and Jarmie 1974, Gillis *et al* 1982).

This forward glory phenomenon has recently been reported (Swenson *et al* 1991) in the decay of an autoionizing state formed by the impact of a slow charged ion. The spectral line shape of the emitted electron is affected by the post-collision interaction with the Coulomb field of the outgoing projectile. The peak is not only broadened and shifted, but also a sharp enhancement of the profile in the direction of the receding ion is observed. Regarding the ideas developed in this paper, this effect can be explained as a forward glory effect. A quantum description (Barrachina and Macek 1989) leads to a maximum in the forward direction, instead of the glory divergence. In addition, an interference structure is predicted. These characteristics of the angular behaviour of the cross section have been observed (Swenson *et al* 1989) in a 10 keV  $\text{He}^+ \rightarrow \text{He}$  collision. A semiclassical model (Swenson *et al* 1989) successfully describes the phenomenon as being due to the interference of the two classical trajectories which are emitted with different emission angles but end up in the same direction  $\Theta$  (see figure 7 and equation (17)). These two orbits go around opposite sides of the outgoing ion.

As a corollary of the ideas presented in this paper, it can be foreseen that a very striking effect might be likely to occur if the autoionizing process were induced by a negatively charged projectile. As a result of a rainbow phenomenon, a deep depletion of electron emission in the forward direction and a sharp enhancement at a certain characteristic emission angle  $\Theta_R$  have to be expected. A quantum description would also show an interference effect which could be related to the supernumerary arcs arising from trajectories that have initial emission angles  $\alpha$  on each side of the rainbow value  $\alpha_R$ . Recently, anomalous oscillations in the binary peak of the electrons emitted in 1 MeV  $\text{amu}^{-1}\text{U}^{+21} + \text{He}$  collisions have also been associated with the phenomena of rainbow and forward glory (Reinhold *et al* 1991).

## Acknowledgments

We wish to thank Verónica Grünfeld for a thorough reading of the manuscript and her very useful suggestions. This work was supported in part by a grant from Fundación Antorchas (Argentina).



## Appendix

It is easy to show that, in the limit  $R \rightarrow \infty$ , the dispersion relation (15) yields the corresponding relation for Rutherford scattering. To do so, we have to define an *impact parameter*  $\rho = R \tan \alpha$ , replace it in equation (15), and take the limit  $R \rightarrow \infty$ . This leads to

$$\rho^2 = \frac{k^2}{m^2 v_\infty^4} \cot^2(\Theta/2), \quad (27)$$

as expected for the scattering of charged particles in a Coulomb field (Landau and Lifshitz 1976).

Furthermore, it is not difficult to relate the differential cross section (20) to our definition (22). First, let us note that  $\alpha = \arctan(\rho/R)$  and only those particles emitted into a narrow forward cone towards the force centre, i.e. the  $\sigma_+(\Theta)$  contribution to the effective cross section, have to be considered. Therefore, we obtain in the limit  $R \rightarrow \infty$

$$\begin{aligned} \frac{d\sigma}{d\Omega} &= \left| \frac{\rho \, d\rho}{d(\cos \Theta)} \right| \\ &= \lim_{R \rightarrow \infty} \left| \frac{\rho \, d\rho}{d(\cos \alpha_+)} \right| \left| \frac{d(\cos \alpha_+)}{d(\cos \Theta)} \right| \\ &= \lim_{R \rightarrow \infty} \frac{R^2}{\cos^3 \alpha} \sigma_+(\Theta), \end{aligned} \quad (28)$$

and, since  $\cos \alpha \rightarrow 1$  when  $R \rightarrow \infty$ , we see that our effective cross section (19) yields the corresponding standard definition equation (20)

$$\frac{d\sigma}{d\Omega} = \left( \frac{k}{2mv_\infty^2} \right)^2 \frac{1}{\sin^4(\Theta/2)}, \quad (30)$$

which is the Rutherford differential cross section for the scattering of a particle by a Coulomb force centre.

## References

- Adolph J W, León García A, Harter W G, McLaughlin G C, Shiffman R R and Surkus V G 1972, *Am. J. Phys.* **40** 1852-7
- Barrachina R O and Macek J H 1989 *J. Phys. B: At. Mol. Opt. Phys.* **22** 2151-60
- Beck D, Ross U and Schepper W 1979 *Phys. Rev. A* **19** 2173-9
- Boyer C B 1959, *The Rainbow: from Myth to Mathematics* (New York: Thomas Yoseloff)
- Bryant H C and Jarmie N 1974 *Sci. Am.* **231** 60-71
- Caplan S, Fuerstenberg H, Hayes C, Kane D and Raboy S 1977 *Am. J. Phys.* **45** 1089-90
- DeVries R M, Goldberg D A, Watson J M, Zisman M S and Cramer J G 1977 *Phys. Rev. Lett.* **39** 450
- Firsov O B 1953 *Zh. Eksp. Teor. Fiz.* **24** 279
- Ford K W and Wheeler J A 1959 *Ann. Phys.* **7** 259-86
- Goldstein H 1965 *Classical Mechanics* (Reading, MA: Addison-Wesley)
- Gillis P, Deleuze C, Henri V P and Lesceux J M 1982 *Am. J. Phys.* **50** 416-21
- Greenler R 1980 *Rainbows, Halos and Glories* (Cambridge: Cambridge University Press)
- Kleyn A W 1987 *Comment. At. Mol. Phys.* **19** 133-51
- Landau L D and Lifshitz E M 1976 *Mechanics* (Oxford: Pergamon)
- Laporte O 1970 *Am. J. Phys.* **38** 837-40
- Manson E 1957 *J. Chem. Phys.* **26** 667-77
- McDowell M R C and Coleman J P 1970 *Introduction to the Theory of Ion-Atom Collisions* (Amsterdam: North-Holland)
- McVoy K W and Satchler G R 1984 *Nucl. Phys. A* **417** 157-73
- Nussenzweig H M 1977 *Sci. Am.* **236** 116-27
- Put L W and Paans A M J 1977 *Nucl. Phys. A* **291** 93
- Reinhold C O, Schultz D R, Olson R E, Kelbach C, Koch R and Schmidt-Böcking 1991 *Phys. Rev. Lett.* **66** 1842-5
- Swenson J K, Burgdörfer J, Meyer F W, Havener C C, Gregory D C and Stolterfoht N 1991 *Phys. Rev. Lett.* **66** 417-20
- Swenson J K, Havener C C, Stolterfoht H, Sommer K and Meyer F W 1989 *Phys. Rev. Lett.* **63** 35-8
- Walker J D 1976 *Am. J. Phys.* **44** 421-33
- Warner R E and Huttar L A 1991 *Am. J. Phys.* **59** 755-6